Tissue factor targeting peptide enhances nanoparticle binding and delivery of a synthetic specialized pro-resolving lipid mediator to injured arteries

Elizabeth S. Levy, PhD,[a,b] Alexander S. Kim, MD,[c] Evan Werlin, MD,[c,†] Mian Chen, MD,[c] Brian E. Sansbury, PhD,[d] Matthew Spite, PhD,[d] Tejal A. Desai, PhD,[a,e] *and* Michael S. Conte, MD,[c] *San Francisco and South San Francisco, CA; Boston, MA; and Providence, RI*

ABSTRACT

Background: Specialized pro-resolving lipid mediators (SPM) such as resolvin D1 (RvD1) attenuate inflammation and exhibit vasculo-protective properties.

Methods: We investigated poly-lactic-co-glycolic acid (PLGA)-based nanoparticles (NP), containing a peptide targeted to tissue factor (TF) for delivery of 17R-RvD1 and a synthetic analog 17-R/S-benzo-RvD1 (benzo-RvD1) using in vitro and in vivo models of acute vascular injury. NPs were characterized in vitro by size, drug loading, drug release, TF binding, and vascular smooth muscle cell migration assays. NPs were also characterized in a rat model of carotid angioplasty.

Results: PLGA NPs based on a 75/25 lactic to glycolic acid ratio demonstrated optimal loading (507.3 pg 17R-RvD1/mg NP; P = ns) and release of RvD1 (153.1 pg 17R-RvD1/mg NP; $P < .05$). NPs incorporating the targeting peptide adhered to immobilized TF with greater avidity than NPs with scrambled peptide (50 nM: 41.6 ± 0.52 vs 32.66 ± 0.34; 100 nM: 35.67 ± 0.95 vs 23.5 ± 0.39; $P < .05$). NPs loaded with 17R-RvD1 resulted in a trend toward blunted vascular smooth muscle cell migration in a scratch assay. In a rat model of carotid angioplasty, 16-fold more NPs were present after treatment with TF-targeted NPs compared with scrambled NPs ($P < .01$), with a corresponding trend toward higher tissue levels of 17R-RvD1 ($P = .06$). Benzo-RvD1 was also detectable in arteries treated with targeted NP delivery and accumulated at 10 times higher levels than NP loaded with 17R-RvD1. There was a trend toward decreased CD45 immunostaining in vessels treated with NP containing benzo-RvD1 (0.76 ± 0.38 cells/mm^2 vs 122.1 ± 22.26 cells/mm^2; $P = .06$). There were no significant differences in early arterial inflammatory and cytokine gene expression by reverse transcription-polymerase chain reaction.

Conclusions: TF-targeting peptides enhanced NP-mediated delivery of SPM to injured artery. TF-targeted delivery of SPMs may be a promising therapeutic approach to attenuate the vascular injury response. (JVS—Vascular Science 2023;4:100126.)

Keywords: Resolution; Inflammation; Specialized pro-resolving lipid mediators (SPM); Resolvin D1 (RvD1); Peripheral arterial disease (PAD); Nanoparticle; Targeted delivery

Peripheral artery disease (PAD) leads to significant decreases in quality of life through pain, impaired mobility, chronic wounds, and amputation.[1] PAD affects 8 to 10 million Americans[2] and more than 200 million people globally.[3,4] Although various techniques exist to improve blood flow in PAD,[5] the durability of these interventions remains a significant limitation; 20% to 50% of patients require repeat interventions within 2 years.

Vascular interventions injure the vessel wall, resulting in the local production of proinflammatory cytokines and leukocyte recruitment. This process induces normally quiescent vascular smooth muscle cells (VSMCs) to

From the Department of Bioengineering and Therapeutics, University of California San Francisco, Department of Anesthesiology, Perioperative and Pain Medicine, Brigham, San Francisco[a]; the Small Molecules Pharmaceutics, Genentech, South San Francisco[b]; the Department of Surgery and Cardiovascular Institute, University of California San Francisco, Department of Anesthesiology, Perioperative and Pain Medicine, Brigham, San Francisco[c]; Women's Hospital and Harvard Medical School, Boston[d]; and the School of Engineering, Brown University, Providence.[e]

†Deceased.

This work was funded by R01 HL119508 U.S. National Institutes of Health, National Heart, Lung, and Blood Institute Grants; University of California Center for Accelerated Innovation (NHLBI Grant Number U54HL119893, and by NIH/NCATS UCSF-CTSI Grant Number UL1 TR001872); Boston Biomedical Innovation Center (B-BIC), U54HL119145; R25 23856 U.S. National Institutes of Health Research Training and Career Development. These institutions had no involvement in the study design or collection, analysis, and interpretation of data and were not involved in the decision to submit the manuscript for publication.

Additional material for this article may be found online at www.jvascsurg.org.

Correspondence: Tejal A. Desai, PhD, Brown University School of Engineering, 184 Hope St, Providence, RI 02912 (e-mail: tejal_desai@brown.edu).

The editors and reviewers of this article have no relevant financial relationships to disclose per the Journal policy that requires reviewers to decline review of any manuscript for which they may have a conflict of interest.

2666-3503

https://doi.org/10.1016/j.jvssci.2023.100126

dedifferentiate, resulting in increased migration, proliferation, resistance to apoptosis, and matrix synthesis. Prolonged pathological inflammation can promote dysfunctional vessel wall remodeling, leading to neointimal hyperplasia (NIH) and recurrent narrowing (restenosis) of the vessel.[6-8]

Resolution denotes the active physiologic termination of inflammation that restores tissue homeostasis. Lipoxygenases and cyclo-oxygenases convert free fatty acid substrates into critical bioactive lipid mediators including prostaglandins and thromboxanes. In animal models of inflammation, lipoxygenase and cyclo-oxygenase activity demonstrate a lipid mediator class switch and begin to convert polyunsaturated fatty acid substrates into an array of signaling molecules known as specialized pro-resolving lipid mediators (SPMs).[9-11] SPMs decrease the production of inflammatory cytokines, decrease leukocyte recruitment, and promote regenerative macrophage M2 polarization.[12-16] Timely transition from inflammation to resolution may limit dedifferentiating signals to VSMCs and attenuate the NIH response after vascular injury.

Resolvin D1 (RvD1; 7S,8 R,17S-trihydroxy-4Z,9 E,11E,13Z,15E,19Z-docosahexaenoic) is an SPM that has demonstrated therapeutic potential in neuropathic pain, arthritis, acute respiratory distress, myocardial infarction, sepsis, and acute kidney injury.[17-21] At the cellular level, our laboratory found that RvD1 decreased rat aortic VSMC proliferation and migration, human VSMC proliferation and migration, and human endothelial cell (EC) p65 nuclear translocation.[22,23] Periadventitial application of RvD1 (using a topical pluronic gel) attenuated NIH in a rat model of carotid angioplasty and in a rabbit model of carotid bypass without observable adverse effects,[22,24] making it a candidate antirestenosis therapeutic.

Effective tissue delivery, stability, and local bioavailability are critical considerations in developing bioactive lipids as therapeutics. Native RvD1 is rapidly degraded by dehydrogenases and reductases.[25] Our group has investigated various avenues to improve SPM durability and delivery. These include 17R-RvD1, a naturally occurring aspirin-triggered epimer of RvD1, and the more recently described 17 R/S-benzo-RvD1 (benzo-RvD1), a synthetically developed RvD1 analog, both of which are more resistant to degradation.[25,26] Treatment with 17R-RvD1 was associated with reduced VSMC migration through cyclic adenosine monophosphate and protein kinase A pathways,[27] and both 17R-RvD1 and benzo-RvD1 decreased NIH in a rat model with topical gel application.[28] We further described a poly-lactic-co-glycolic acid (PLGA)-based film device with unidirectional release of RvD1, which achieved good SPM delivery and reduced NIH, but this approach is limited to an open surgical environment.[24] The present work investigates a carrier with potential for catheter-based applications.

ARTICLE HIGHLIGHTS

- **Type of Research:** Rat model, in vitro study
- **Key Findings:** In vitro experiments characterized a novel tissue factor targeted nanoparticle (NP) loaded with specialized pro-resolving lipid mediators (SPM). Incorporation of the targeting peptide resulted in improved NP binding during in vitro and in vivo models of vascular injury, associated with a trend toward increased delivery of SPM and reduced leukocyte recruitment.
- **Take Home Message:** These studies demonstrate that tissue factor targeting peptide enhances NP binding and SPM delivery to injured arteries, and that targeted NPs are a promising platform for delivery of SPM to attenuate the vascular injury response.

Nanoparticles (NPs) are a powerful tool to deliver therapeutic compounds to specific areas of the body or sites of disease.[29,30] NPs can encapsulate small payloads and decrease degradation.[31] NPs can also be modified for targeting, maximizing therapeutic concentrations at desired regions while limiting off-target side effects and systemic circulation.[32,33] A tissue factor (TF) targeting peptide was published in a study using prothrombotic nanofibers to control hemorrhage.[34] TF, a protein exposed to the circulation only after vascular injury, is an ideal target because it provides specificity in the setting of vascular intervention.

Combining the pro-resolving effects of SPMs, the stability and clinical versatility of NPs, and a targeting mechanism specific to vascular injury, we have developed NPs capable of delivering RvD1 to injured vasculature (Fig 1, *A*). The objective of this study was to test the feasibility of these NPs for safety, specificity to binding TF and areas of vascular injury, and their therapeutic potential in various models of vascular inflammation and injury.

METHODS

Reagents, cells, and treatment protocol. Human great saphenous veins discarded at the time of coronary or peripheral bypass grafting at The University of California-San Francisco (approved by the Institutional Review Board; UCSF Committee on Human Research Number: 10-03,395; the committee waived the need for informed consent) were used to prepare primary cultures of EC and VSMC, as described previously.[35] All cells were used between passages 2 and 5.

The RvD1 analog, benzo-RvD1 ($C_{22}H_{30}O_5$), was prepared by custom total organic synthesis by Cayman Chemical (Ann Arbor, MI). 17R-RvD1 was purchased from Cayman Chemical.

Targeting peptide-polymer conjugation. The TF targeting peptide sequence was {Lys(FITC)}CGGGKFRVFALTR; a

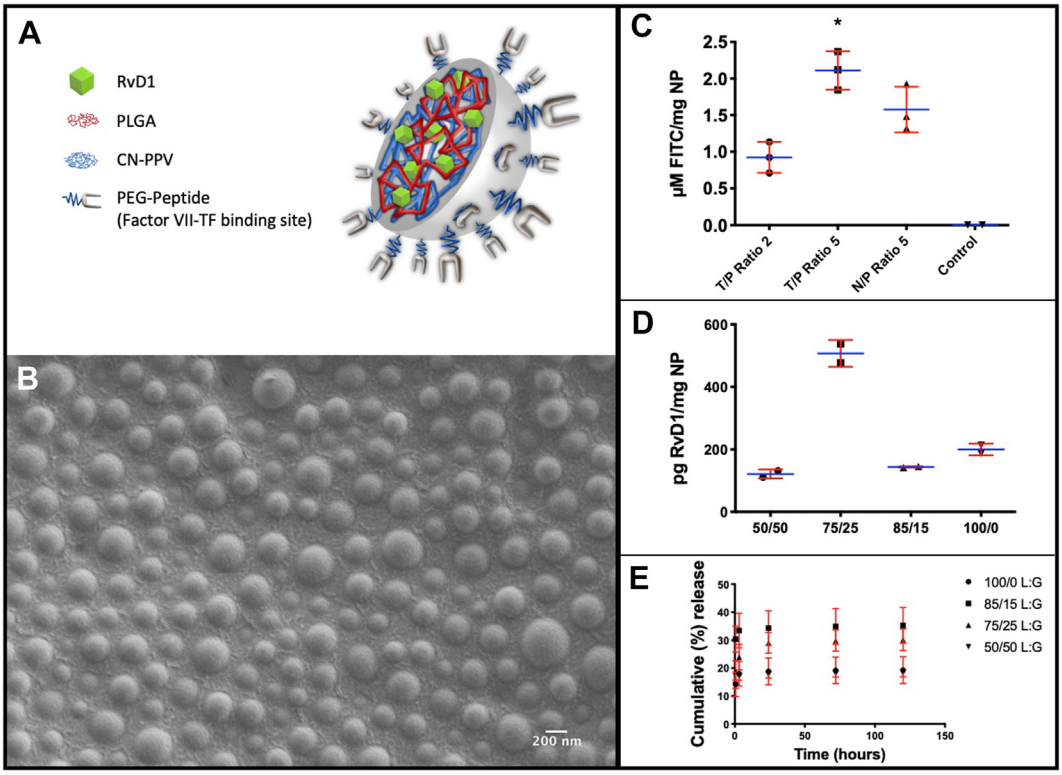

Fig 1. Tissue factor (TF)-targeted poly-lactic-co-glycolic acid (*PLGA*) nanoparticles (*NP*), peptide incorporation, and resolvin D1 (*RvD1*) loading and release. **(A)** Schematic of PLGA NP with targeting peptide and RvD1 loading. Poly(2,5-di(hexyloxy)cyanoterephthalylidene (*CN-PPV*) is an inert fluorescent polymer included on the NP for visualization during experiments. **(B)** Scanning electron microscopy image of NPs. **(C)** Peptide loading into NPs as a function of the ratio of peptide to PLGA (n = 2 for control, n = 3 for all other groups; *$P < .05$ compared with control). Ratios of targeted (*T*) or scrambled (*N*) to PLGA-PEG-maleimide ranging from 2 to 5 are shown. Friedman test, Dunn's post hoc. **(D)** RvD1 loading into PLGA NPs. Various NP ratios of lactic:glycolic acid are shown (n = 2 for all groups; *P* = ns). Friedman test, Dunn's post hoc. © In vitro elution of RvD1 from PLGA NPs. The effect of various ratios of lactic:glycolic (*L:G*) acid on cumulative release of RvD1 over 120 hours is shown (n = 3 for all groups; *$P <$ .0001 compared with all other ratios). Two-way analysis of variance (ANOVA), Tukey's post hoc test. Blue lines represent means, red bars represent standard deviations.

randomized sequence of the same amino acids was used for the scrambled peptide control {Lys(FITC)} CGGGARVFTFRLK.[34] The TF-targeting and scrambled peptide were first conjugated to PLGA-polyethylene glycol (PLGA-PEG)-maleimide 10k-5k (PolySci Tech, West Lafayette, IN). Two molar ratios were tested (2:1 and 5:1 of peptide to PLGA-PEG-maleimide polymer ratios); the peptide was added to the PLGA-PEG-maleimide (30 mg/mL) in dimethylformamide with 6% v/v triethylamine. The mixture was reacted overnight to conjugate the thiol of the cysteine on the peptide to the PLGA-PEG-maleimide, and the dimethylformamide was evaporated by high spin vacuum. Samples were stored at −20°C.

NP production. A solution consisting of 100 mg of 100/0, 85/15, 75/25, or 50/50 lactic acid/glycolic acid (L/G) ratio of poly(lactic-co-glycolic acid) (PLGA) in dichloromethane (50 mg/mL) and poly(2,5-di(hexyloxy)cyanoterephthalylidene (CN-PPV) (3.25 mg/mL) in chloroform (Sigma-Aldrich, St Louis, MO) was combined. RvD1 (200 ng), 17R-RvD1 (200 ng), or benzo-RvD1 (2000 ng) were added to NPs in ethanol. For NPs with the peptide on the surface, either targeting or scrambled peptide conjugated to PLGA-PEG-maleimide (20 nmol) was added to 50 mg of PLGA and 3% (w/v) polyvinyl alcohol (PVA) was added at a 1:2 ratio of polymer solution to 3% PVA (v/v). The solution was probe sonicated on ice at 7 to 8 W or 30 amplitude for 5 seconds on and 10 seconds off for a total of 5 cycles, resulting in stable NPs. The NP solution was then diluted 10 times with 0.3% (w/v) PVA and stirred for 2 hours to evaporate the dichloromethane, followed by purification with a soft wash at 500 rpm to remove large aggregates. Finally, the NPs were washed three times with 1% (w/v) PVA and centrifuged at 12,500 rpm for 10 minutes to remove undersized NPs and unencapsulated drug. The NPs were lyophilized and stored at −80°C. Before the studies, the NPs were resuspended in phosphate-buffered saline (PBS) or 10% fetal bovine serum Dulbecco's Modified Eagle's Medium (DMEM).

Total payload and release studies. The functional experiments were performed with 17R-RvD1, which is therapeutically active, whereas the release and loading was determined with 17S-RvD1 because an enzyme-linked immunosorbent assay (ELISA) is commercially available (Cayman Chemical). Maximum loading of RvD1 or benzo-RvD1 in the NPs was measured by dissolving the NPs in 1M NaOH. The solution was neutralized with HCL and diluted with 10× PBS. The samples were analyzed by ELISA for RvD1 or liquid chromatography tandem mass spectrometry (LC-MS/MS) for benzo-RvD1 (see below).

SPM release from drug-loaded NPs was evaluated with PBS as an elution buffer. NPs were incubated at 37°C with 400 μL of PBS in Eppendorf tubes while shaking. The tubes were scarified, and the amount of RvD1 or benzo-RvD1 in the supernatant was measured at 30 minutes, 3 hours, 9 hours, and 1, 3, and 5 days. Samples were analyzed accordingly by ELISA or LC-MS/MS (discussed elsewhere in this article).

Targeting peptide loading and binding assay. The targeting peptide was tagged with fluorescein isothiocyanate to quantify incorporation into the NPs. Varying ratios of targeted peptide to PLGA-PEG-maleimide (T/P) and scrambled peptide to PLGA-PEG-maleimide (N/P) were used to characterize the effect of peptide to PLGA-PEG-maleimide ratio on the loading of peptide onto NPs. The fluorescein isothiocyanate fluorescence was measured with a plate reader at ex/em 490/525 nm.

For binding assays, a 96-well plate was incubated with varying concentrations of TF (50-500 ng/well) to precoat the wells for 2 hours at 37°C and overnight at 4°C. Before the experiments, the fluid was aspirated from wells and the plate was dried for 1 hour. Targeted and scrambled NPs were incubated in wells for 10 minutes. The wells were rinsed to remove unbound NPs and fluorescence was quantified at ex/em 490/525 nm. A positive control group was added (peptide control), containing fluorescently labeled targeting peptide without NPs.

Cell viability (PrestoBlue). VSMCs and ECs were seeded at 1×10^4 cells in a 96-well plate containing 10% serum medium and incubated with NP loaded with 17R-RvD1 and soluble 17R-RvD1 at various concentrations, along with a no treatment group. Cells were treated for 24 hours before performing the viability assay. The media were removed, and PrestoBlue cell viability Reagent (Invitrogen, Waltham, MA) was added to the wells for 10 minutes at 37°C. Absorbance was read at 570 nm. Wells lacking NPs and 17R-RvD1 were used as controls.

Cell migration. VSMCs were grown to confluence on 24-well plates. After overnight serum starvation, a linear mechanical wound was made across the center of each well with a 200-μL pipette tip. Detached cells were removed with PBS. Cells were exposed to fresh 0.5% DMEM with no agonist (negative control) or platelet-derived growth factor subunit B (10 ng/mL; Sigma-Aldrich). We added 17R-RvD1 (0.1 nM − 100 nM), NPs loaded with 17R-RvD1, unloaded NP, or PVA to appropriate wells before treatment with agonist. NP are lyophilized in PVA to stabilize the particles and reduce aggregation. They are subsequently re-suspended in deionized water for dosing; as a result, PVA remains the most relevant vehicle control. VSMC cultures were photographed with 10× power at baseline and at 16 hours after the scratch was performed, and wound closure was quantified by ImageJ. Each treatment was repeated in four wells and two 10× power fields were photographed per well.

ECs were grown to confluence on 24-well plates that were coated with 1% gelatin and allowed to dry before plating. After overnight serum deprivation with 0.5% fetal bovine serum media, the mechanical scratch was made as described elsewhere in this article, followed by a gentle rinse with PBS. Fresh 0.5% DMEM containing soluble 17R-RvD1 (0.1-100.0 nM), NPs loaded with 17R-RvD1, unloaded NPs, or PVA (vehicle control) were added to appropriate wells. Platelet-derived growth factor subunit B (10 ng/mL; Sigma-Aldrich) was added as the migration inducing agonist, except in the negative control wells. Wounds were observed at baseline and at 16 hours, and wound closure was quantified by ImageJ. Each treatment was repeated in four wells and two 10× power fields were photographed per well.

Rat carotid artery injury model. Experiments were humanely performed on Sprague-Dawley rats (350-500 g; $n = 38$) with Institutional Animal Care and Use Committee approval (University of California, San Francisco #AN171612). As previously described, the left common carotid artery was injured by balloon angioplasty.[22] Rats were anesthetized with buprenorphine, isoflurane, and lidocaine. After clamping the external, internal and proximal common carotid arteries, a 2F embolectomy balloon (Edwards Lifesciences, Irvine, CA) was inserted retrograde through an arteriotomy on the external carotid artery and inflated in the common carotid artery at 5 atm for 1 minute with a calibrated insufflator (Boston Scientific, Marlborough, MA). After angioplasty, 100 μL of NP solution (with concentration equivalent to 80 nM benzo-RvD1 or 100 nM 17R-RvD1) or PVA (vehicle control) were instilled in the common carotid artery with a 30G needle for 10 minutes with flow occlusion. The artery was flushed by unclamping the common carotid artery, the external carotid artery ligated, and flow restored to the internal carotid artery. Rats were euthanized after 10 minutes or 3 days, and the carotid arteries were perfused with heparinized saline and harvested. One-third of the artery was frozen in optimal cutting temperature compound, one-third was preserved in RNAlater, and the final third was processed for LC-MS/MS to measure 17*R*-RvD1 and benzo-RvD1, as described elsewhere in this article.

Targeted LC-MS/MS. Targeted LC-MS/MS was used to measure 17*R*-RvD1 and benzo-RvD1 in NP or vascular tissue. For this process, internal deuterium-labeled standards, including d_5-resolvin D2 (Cayman Chemical), were added to assess extraction recovery. Solid-phase extraction and LC-MS/MS analysis were carried as previously described.[36] Lipid mediators were extracted by C18 column chromatography, and methyl formate fractions were taken to dryness under a stream of N_2 gas before suspension in methanol:water (50:50). Samples were analyzed using a high-performance liquid chromatograph (Shimadzu, Kyoto, Japan) coupled to a QTrap5500 mass spectrometer (Sciex, Framingham, MA). The instrument was operated in negative ionization mode, and lipid mediators were identified and quantified using multiple reaction monitoring transitions specific for 17*R*-RvD1 (375/215) and benzo-17 *R*/*S*-RvD1 (373/141, 373/213).[26] Information-dependent acquisition and enhanced product ion scanning enabled analysis of full MS/MS spectra to confirm compound identity in selected samples. Lipid mediators were quantified by interpolation based on linear external calibration curves for each mediator using authentic standards and by normalization to extraction recovery based on internal deuterium-labeled standards.

Immunostaining and fluorescence microscopy. We took 6-μm frozen sections of the harvested arteries throughout the zone of injury. Frozen sections were fixed in acetone or 4% paraformaldehyde for 10 minutes before staining. Sections were then permeabilized with 0.2% Triton-X (Sigma-Aldrich). The remaining steps were performed using Tyramide SuperBoost Kit (Invitrogen). Sections were blocked in 10% goat serum. Endogenous peroxidase activity was quenched with 3% H_2O_2. Blocking of endogenous avidin/biotin was performed with a commercial kit (Vector Laboratories, Burlingame, CA) before incubation with one of the following primary antibodies: Ki67 (1:2000; Abcam AB16667), CD45 (1:2000; Abcam AV10558), or (1:1000; Abcam AB9535), followed by incubation with a poly-horseradish peroxidase-conjugated secondary antibody and tyramide working solution. Alexa-Fluor 488 was applied to fluorescently label the secondary antibody (1:200; Invitrogen) and DRAQ7 (1:100; BioLegend, San Diego, CA) was used to stain nuclei. Sections were mounted with Fluoromount-G solution (SouthernBiotech, Birmingham, AL).

Images (three sections per artery) were obtained at 20× magnification with a Nikon Widefield Epifluorescence microscope. Images were analyzed via ImageJ software. The intima/media was selected freehand, and the nuclei, antibody, and NP channels were separated. The degree of NP binding was represented as a ratio of NP fluorescence to total intima/media areas. Areas of overlap nuclei/antibody overlap were designated as positive cells. The number of positive cells was normalized to total intima/media area in mm^2.

Reverse transcription-polymerase chain reaction. Total RNA was isolated from harvested arteries using the RNeasy Micro Kit (Qiagen, Germantown, MD) with RNase-free DNase treatment according to the manufacturer's protocol. Total RNA from each specimen was used to generate cDNA using the High-Capacity cDNA Reverse Transcription Kit (Applied Biosystems, Foster City, CA) for subsequent reverse transcription-polymerase chain reaction reactions. Amplification of DNA was detected by incorporation of SYBR Green (Applied Biosystems). Dissociation curve analyses were performed to confirm the specificity of the SYBR Green signal. Data were normalized to two reference genes and subsequently to PVA (vehicle)-treated arteries. PCR parameters included an initial 10-minute denaturation step at 95°C, followed by a cycling program of 95°C for 10 seconds and 60°C for 30 seconds for 40 cycles (CFX96 Real-Time System; Bio-Rad, Hercules, CA). IL-6 (AGCGATGATGCACTGTCAGA, TCCAGAAGACCAGAGCAGAT), IL-10 (CCCTCTGGATACAGCTGCGA, ATGGCCTTGTAGACACCTTTGT), HO-1 (ACAGAGTTTCTTCGCCAGAGG, GGTCGCCAACAGGAAACTGA), and MCP-1 (GCCTGTTGTTCACAGTTGCT, GTTCTCCAGCCGACTCATTG) were analyzed.

Statistical analyses. The Shapiro-Wilk test was used to determine normality. For data sets that were normal, one-way analysis of variance (ANOVA) was used for initial multigroup analyses, followed by Tukey's post hoc pairwise group comparisons. For non-normal data, the Friedman test followed by the Dunn test were used to determine statistical significance. Unpaired *t* test assuming unequal variances was used for data comparing two groups if the data were parametric. If data were nonparametric, then the Mann-Whitney *U* test was used. The threshold for statistical significance was set at a *P* value of $<.05$. All data shown in graphs are presented as dot-plots with the error bars representing standard deviations.

RESULTS

NP production and targeting peptide loading. PLGA NPs have been designed with modular functional groups on the surface for selective delivery of NPs encapsulating drug molecules to the target tissues.[37] We hypothesized that encapsulating RvD1 in TF-targeted NPs would concentrate the delivery of SPMs at the vascular injury site. To develop TF-targeted NPs, we used PLGA, which has biocompatible and biodegradable properties, to encapsulate RvD1. NPs were synthesized by single emulsion sonication with the addition of a fluorescent polymer, CN-PPV, to enhance in vivo visualization and tracking (Fig 1, *A*). By scanning electron microscopy and dynamic light scattering, the produced NPs measured

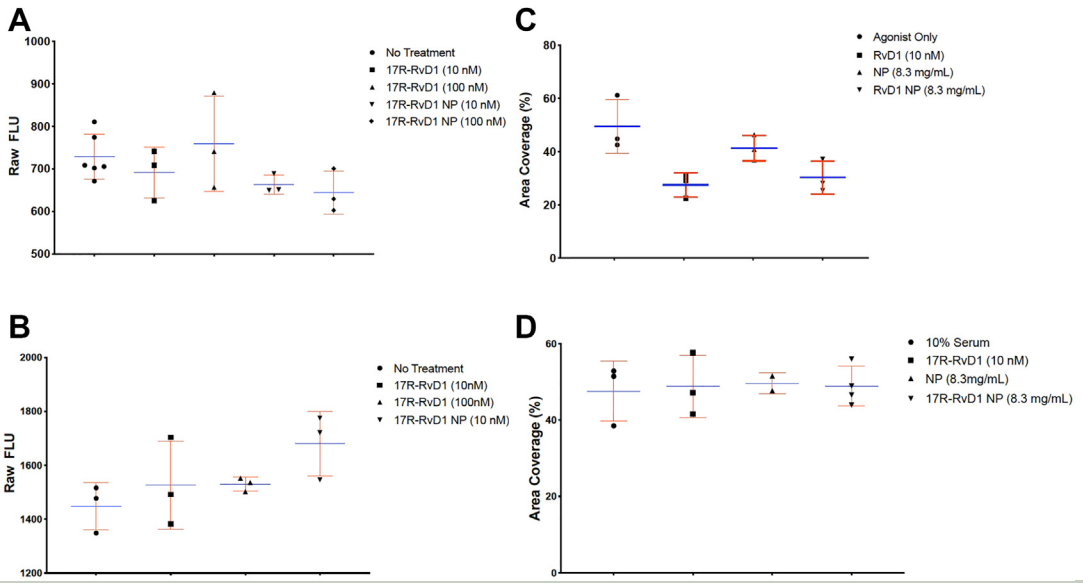

Fig 2. Vascular smooth muscle cell (VSMC) and endothelial cell (EC) viability and migration. **(A)** Results from Prestoblue assay demonstrating VSMC viability after exposure to free soluble 17R-resolvin D1 (*RvD1*) and 17R-RvD1-loaded NPs. (n = 6 for no treatment, n = 3 for all other groups.) **(B)** Results from Prestoblue assay demonstrating EC viability after exposure to free soluble 17R-RvD1 and 17R-RvD1-loaded NPs. (n = 3 for all groups.) **(C)** Results from scratch assay demonstrating the effect of platelet-derived growth factor subunit B (migration agonist only positive control), free soluble 17R-RvD1, nanoparticles (*NP*), and 17R-RvD1-loaded NP on VSMC migration (n = 3 for all groups.) **(D)** Results from scratch assay demonstrating the effect of free soluble 17R-RvD1, NP, and 17R-RvD1-loaded NP on EC migration (n = 3 for all groups). All figures used the Friedman test, which resulted in P = ns. Blue lines represent means, red bars represent standard deviations.

259.6 ± 18.1 nm with a polydispersity index of 0.099 (Fig 1, *B*). Increasing ratios of peptides to PLGA NPs increased peptide loading (*$P < .05$ compared with control). The T/P ratio 2 is 2:1 peptide to PLGA-PEG-maleimide ratio, and ratio 5 is 5:1 peptide to PLGA-PEG-maleimide ratio. The scrambled control peptide (N/P ratio 5) incorporated similarly to the targeted peptide (T/P ratio 5) (Fig 1, *C*).

L/G ratio of 75/25 results in optimal RvD1 loading. Altering the L/G ratio of PLGA affects the loading and release owing to polymer hydrophobicity and increased polymer degradation at greater concentrations of glycolic acid.[38] PLGA with L/G ratio of 75/25 provided the highest amount of RvD1 loading ($P < .001$) (Fig 1, *D*) and RvD1 release ($P < .01$) over time (Fig 1, *E*). The loading of RvD1 was 0.5 ng/mg NP with an encapsulation efficiency of 25%. As a result, the 75/25 L/G ratio PLGA polymer was used for all subsequent experiments. The loading of benzo-RvD1 was 0.37 ± 0.03 ng/mg of NPs. The NP release of benzo-RvD1 into elution buffer was stable out to 5 days (3 hours, 37.07 ± 1.7 pg/μL; 9 hours, 37.92 ± 1.2 pg/μL; 3 days, 36.62 ± 2.43 pg/μL; 5 days, 41.96 ± 2.21 pg/μL).

NPs loaded with 17R-RvD1 associated with trend toward reduced VSMC migration. Exposure to NPs did not affect EC or VSMC viability (Figs 2, *A* and *B*). The 17*R*-RvD1 loaded NPs at 8.3 mg/mL, equivalent to 10 nM of free 17R-RvD1, demonstrated a trend toward reduced VSMC migration compared with unloaded NP (% area coverage 49.52 ± 10.2 and 41.4 ± 4.8 for agonist control and bland NP vs 27.5 ± 4.6 and 30.6 ± 5.8 for free RvD1 and RvD1 NP; P = ns) (Fig 2, *C*). Neither 17R-RvD1, the NP, nor the loaded NP affected EC migration (Fig 2, *D*).

Targeting peptide improves NP binding to TF in vitro. Using an in vitro binding assay, we examined the effects of NP targeting, NP concentration, and TF precoat concentration. There was a significant increase in targeted NP vs scrambled NP binding at the highest two doses of NP tested with a fixed concentration of immobilized TF of 500 ng per well (50 nM, 41.6 ± 0.91 vs 32.66 ± 0.59; 100 nM, 35.67 ± 1.65 vs 23.5 ± 0.67; $P < .05$) (Fig 3, *A*). Targeted NP binding efficacy was increased with increasing concentrations of immobilized TF, being highest in wells coated with 500 ng and 250 ng of TF (250 ng, 15.58 ± 2.74 vs 9.66 ± 1.42 [$P < .05$]; 500 ng, 23.17 ± 3.02 vs 17.09 ± 2.46 [$P = .0539$]) (Fig 3, *B*).

Targeting peptide improves NP binding to injured arteries and increases tissue SPM delivery. A total of 38 rats were used for this study. There were two cases of carotid artery thrombosis (5.3%) and one case of neck hematoma (2.6%) causing respiratory distress, which led to early sacrifice. These cases did not correlate with treatment and they were excluded from analysis, resulting in a final n = 35.

In the rat model of balloon carotid injury, we observed a 16-fold greater NP fluorescence in tissue harvested 3 days

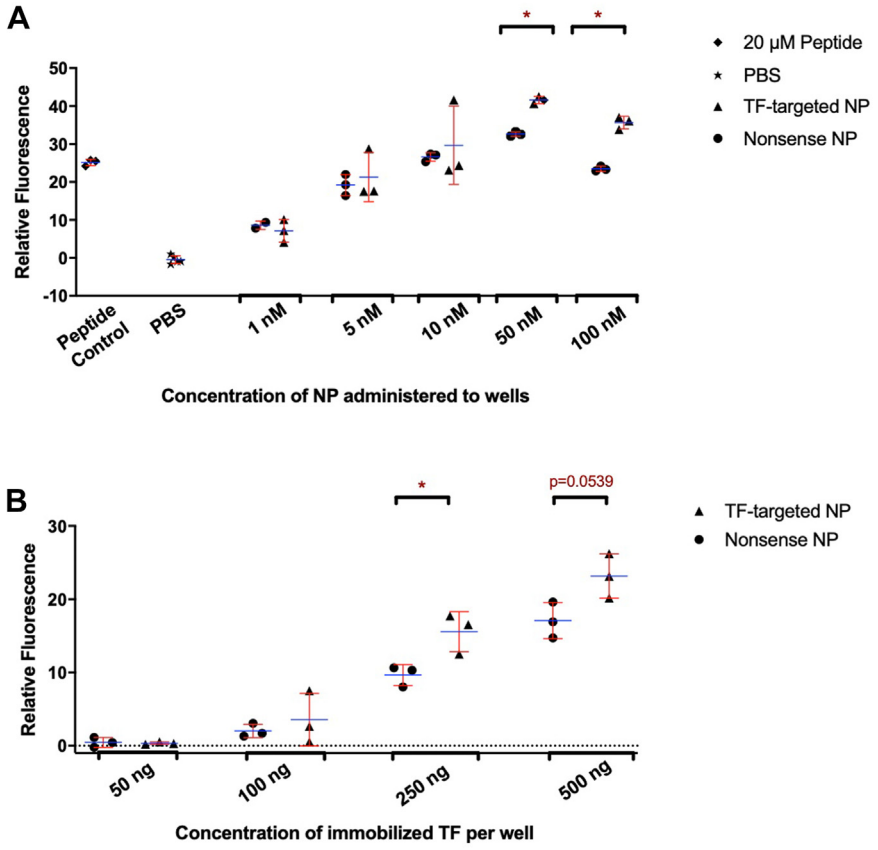

Fig 3. In vitro targeted nanoparticle (*NP*) binding assays. **(A)** NP binding assay demonstrating the effect of administering increasing concentrations of targeted NP to wells precoated with 500 ng of immobilized tissue factor (*TF*) (n = 3 for all groups; **P* < .05). **(B)** NP binding assay demonstrating the effect of varying the concentration of immobilized TF in wells treated with 100 nM targeted NP (n = 3 for all groups; **P* < .05). All figures used one-way analysis of variance (ANOVA) with Tukey's post hoc test. Blue lines represent means, red bars represent standard deviations. *PBS*, phosphate-buffered saline.

after treatment with targeted NP (n = 8) vs scrambled NP (n = 4) (area ratio compared with intima/media of 0.01 ± 0.005 vs 0.0006 ± 0.0007; *P* < .01) (Figs 4, *A* and *B*).

There were corresponding, although not statistically significant, higher tissue levels of 17R-RvD1 in injured arteries treated with targeted NPs compared with scrambled NPs (0.232 ± 0.15 pg/mg vs 0.00 ± 0.00 pg/mg; *P* = .06) by LC-MS/MS analysis at acute sacrifice (Fig 4, *C*). We also identified benzo-RvD1 in arteries treated with targeted NP loaded with benzo-RvD1 (2.10 ± 1.24 pg/mg; n = 3). The levels of benzo-RvD1 achieved in the tissue after acute sacrifice were nearly 10-fold higher than that after 17R-RvD1-NP treatment (0.232 ± 0.09 pg/mg; n = 3); thus, further in vivo experiments were performed with benzo-RvD1.

NP delivery of benzo-RvD1 is associated with a trend toward reduced early leukocyte recruitment. Arteries harvested 3 days after injury were examined for CD45 as a pan-leukocyte marker for early inflammatory cell recruitment. Arteries treated with vehicle (PVA) without NPs demonstrated 59.31 ± 32.02 $CD4^{(+}$ cells/mm^2 (of note, one outlier value was removed from this group as it was >1.5 × the interquartile range above the third quartile), whereas arteries treated with unloaded (blank) targeted NPs contained 122.1 ± 62.9 $CD45^+$ cells/mm^2 (Figs 5, *A* and *B*). Arteries treated with targeted benzo-RvD1 NP demonstrated a nonsignificant trend toward lower $CD45^+$ counts, as did those treated using scrambled NPs loaded with benzo-RvD1 (0.76 ± 0.76 and 8.9 ± 2.41 vs vehicle 59.31 ± 32.02 and targeted control 122.1 ± 62.9; *P* = ns). We observed a trend toward reduced myeloperoxidase staining in arteries treated with benzo-RvD1, but this did not achieve significance (vehicle 33.2 vs targeted blank 80.8 vs scrambled benzo 25.2 vs targeted benzo 13.4 positive nuclei/mm^2, ANOVA; *P* = .055) (Supplementary Fig, *A*). There was no significant difference in staining for the proliferation marker Ki67 at POD3 (vehicle 106.3; targeted blank 138.0; scrambled benzo 70.2; targeted benzo 76.3 positive nuclei/mm^2, ANOVA; *P* = .81) (Supplementary Fig, *B*).

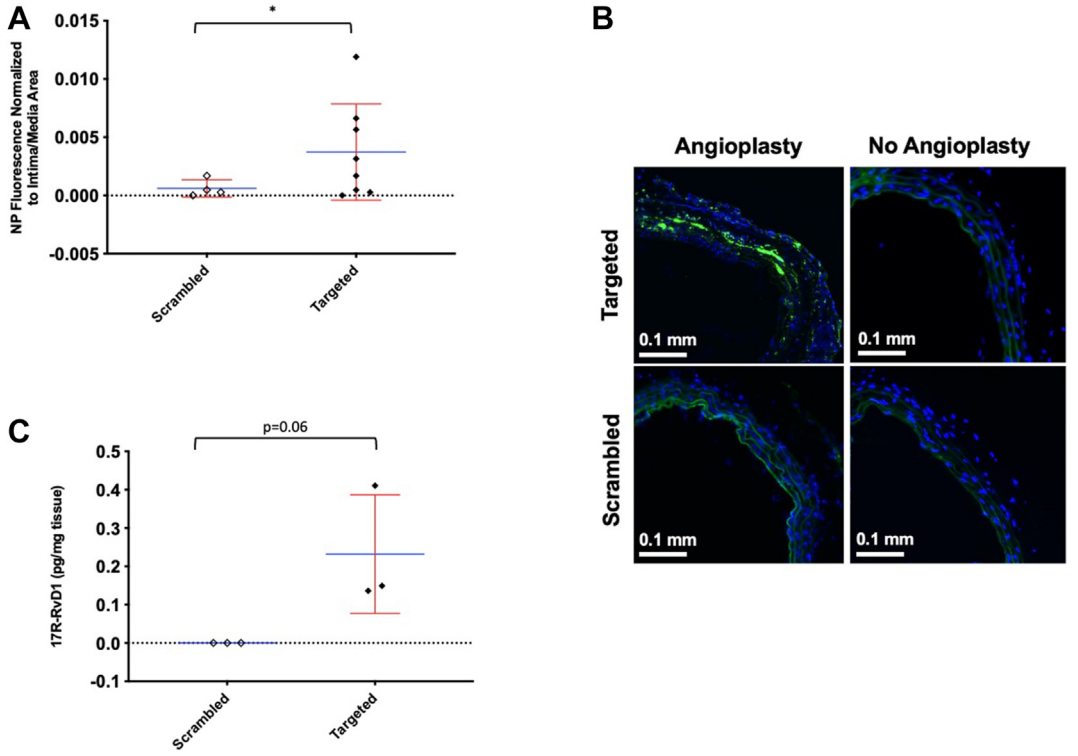

Fig 4. In vivo nanoparticle (*NP*) targeting and benzo-resolvin D1 (*RvD1*) delivery. **(A)** Quantification of scrambled and targeted NP binding following administration after carotid artery injury (n = 4 for scrambled, n = 8 for targeted; $P < .001$). Unpaired *t* test assuming unequal variance. (B) Representative images of rat carotid artery with/without injury and after exposure to targeted or scrambled NPs. Blue represents nuclei, green represents NPs. **(C)**. Liquid chromatography tandem mass spectrometry (LC-MS/MS) analysis measuring 17R-RvD1 in tissue after injury and administration of 17R-RvD1-loaded targeted NPs immediately after injury (n = 3 for both groups; $P = .06$). Mann—Whitney *U* test. Blue lines represent means, red bars represent standard deviations.

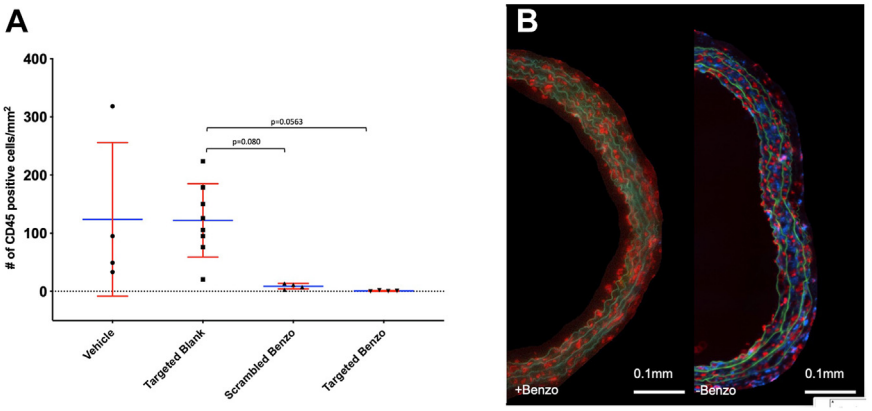

Fig 5. CD45 staining of injured arteries at postoperative day (POD) 3 after administration of nanoparticles (NPs). **(A)** Quantification of CD45 staining in injured arteries at POD 3 after administration of vehicle (polyvinyl alcohol [PVA]) and various NPs (n = 3 for vehicle; n = 8 for targeted blank; n = 4 for all other groups). One-way analysis of variance (ANOVA), Tukey's post hoc test. Blue lines represent means, red bars represent standard deviations. **(B)** Representative images demonstrating reduced CD45 staining (blue) in the artery treated with NPs loaded with benzo-resolvin D1 (RvD1). Red represents nuclei, blue represents CD45 staining, and green represent autofluorescence and/or NP.

NP treatment did not affect early inflammatory gene or cytokine expression. There were no significant differences observed in IL-6, IL-10, HO-1, or MCP-1 expression (by quantitative RT-PCR) at postoperative day 3.

DISCUSSION

Despite the availability of various surgical and endovascular treatments for peripheral arterial disease, these interventions are limited by prolonged inflammation, NIH, and clinical restenosis.[6] Failure rates are higher after endovascular treatments such as angioplasty or stenting compared with more invasive open interventions such as bypass or endarterectomy.[39,40] Current therapeutic approaches to attenuate restenosis are limited. Paclitaxel is a commonly used antiproliferative chemotherapeutic agent that inhibits VSMC proliferation; however, it has significant adverse effects on endothelial healing, which necessitates the use of antiplatelet drugs.[41] Hence, there is an ongoing search for alternative approaches.

Researchers have studied the role of SPMs in various pathologies to investigate their potential for clinical applications.[12,42,43] There are several classes of SPMs, including D- and E-series resolvins, protectins, maresins, and lipoxins.[42,44] These SPMs have been beneficial in the setting of various animal models of inflammatory pathologies, including periodontitis, peritonitis, atherosclerosis, and vascular injury.[22,45-47]

Prior small animal studies have investigated SPMs in models of NIH and limb ischemia-reperfusion injury, but the method of administration has largely been limited to nonspecific intraperitoneal, intravenous, and subcutaneous delivery.[23,48-51]

The importance of efficient and precise delivery of therapeutics is widely recognized in the field of cardiovascular medicine. Current approaches, including the use of balloon catheters, stents, or endovascular needles, can be technically challenging and paradoxically induce further vascular injury, inflammation, and, in the case of stents, a prolonged foreign body inflammatory response.[52,53]

In response to these issues, we have encapsulated SPMs in a single emulsion to form stable PLGA NPs capable of targeting acutely injured arteries with small molecules, including bioactive lipids. Targeted NPs represent a controlled formulation that can be applied to a broad range of platforms and clinical scenarios. PLGA is an ideal polymer because it is biodegradable, nontoxic, and US Food and Drug Administration-approved for use in vascular drug delivery.[54,55] TF was the chosen target because it is a subendothelial protein exposed to the circulation only after vascular injury. The targeting peptide used in this study was the binding site of factor VII, as previously described by Morgan et al.[34] This group used the targeting peptide to control hemorrhage in a mouse model of liver punch biopsy. This specific peptide sequence resulted in both binding at the site of biopsy, as well as reduced hemorrhage. We hypothesized that TF targeting would allow the NPs to bind exclusively to sites of vessel injury. Theoretically, there is a risk of coagulation interference with TF binding. However, only the TF exposed to NPs at the time of treatment would be affected. The risk of hemorrhage at an angioplasty site is low, and bleeding risk is associated with the vascular access/puncture site, which is remote from the location of angioplasty. We observed no hemorrhagic complications. RvD1 was selected owing to the commercial availability of ELISA tests, as well as our prior in vitro and in vivo data. Further experiments were conducted with the synthetic analogue benzo-RvD1 owing to improved shelf life and in vivo stability.[26]

There have been previous efforts exploring the targeted delivery of pro-resolving agents in the literature, including use of a PLGA-PEG-based NP targeted to type IV collagen containing a pro-resolving peptide derivative of annexin A1 in a murine atherosclerosis model,[56] and NPs containing AT-RvD1 and LXA_4 in a murine model of chemical peritonitis.[57] This work is the first instance of using TF-targeted NPs to deliver SPMs after vascular injury.

Our findings indicate that PLGA NPs are nontoxic to vascular cells, and that 75/25 is an optimal ratio of L/G for loading and release of RvD1. NP elution of RvD1 was associated with a trend toward reduced VSMC migration to a similar degree as soluble RvD1 administration. TF targeting peptide increased local binding of NPs both in vitro and in vivo, with a corresponding increase in residual amounts of RvD1 in arteries at acute sacrifice. We observed higher tissue levels of benzo-RvD1 compared with 17R-RvD1 after treatment, which led us to conduct further in vivo experiments with benzo-RvD1. Benzo-RvD1 via NP was associated with a trend toward reduced leukocyte recruitment, but this finding was independent of targeting. Given these results, additional research is required to confirm the benefit of targeted NP delivery of SPMs; however, targeted and more durable delivery generally result in improved clinical benefit.[30,31]

Our study has several limitations. The optimal pharmacokinetics to modulate the acute inflammatory response and downstream clinicopathological effects is unclear. Although the concentration and volume of NP solution was consistent, precise quantification of NP deposition is challenging. For experiments using human cells from various donors, it is possible that interdonor variability could have impacted results, but all experiments included in this study used a single donor per experiment to decrease variability. Although all balloon injuries were performed as uniformly as possible, endothelial disruption may be nonuniform, which influences the binding of NPs. We had two thrombosis events that were likely related to technical errors/seroma that compressed or caused stenosis of the carotid artery, leading to thrombosis. The coagulation cascade is identical in

rats and humans; TF interacts with factor VII to initiate the extrinsic pathway of coagulation. Any interaction with the NP would lead to localized impairment in coagulation rather than thrombosis. Off-target binding of the NPs or the duration of PLGA NPs in the tissue are important data that need further investigation. This was an early feasibility study, and not adequately powered for downstream end points such as gene expression, tissue remodeling, and NIH.

CONCLUSIONS

PLGA NP with L/G ratio 75/25 provided efficient loading of SPM. Incorporation of TF targeting peptide improved PLGA NP binding to TF in vitro and to acutely injured arteries. This corresponded with improved local delivery of RvD1 in a rat model of carotid angioplasty. Intraluminal delivery of benzo-RvD1 via NPs, regardless of targeting, was associated with a trend toward reduced leukocyte recruitment after carotid angioplasty, which was not statistically significant. Benzo-RvD1 NPs represent a candidate formulation of therapeutic SPM to reduce vascular inflammation at clinically relevant sites of vascular injury. Further efforts are necessary to identify pharmacokinetic requirements, optimization of formulations, and measure the downstream effects of targeted SPM NPs on longer term inflammatory and NIH response in appropriate animal models.

AUTHOR CONTRIBUTIONS

Conception and design: TD, MSC
Analysis and interpretation: EL, AK, EW, BS, MS, TD, MSC
Data collection: EL, AK, EW, MCh, BS, MS
Writing the article: EL, AK, EW, TD, MSC
Critical revision of the article: EL, AK, MCh, BS, MS, TD, MSC
Final approval of the article: EL, AK, EW, MCh, BS, MS, TD, MSC
Statistical analysis: EL, AK, EW, MCh, BS, MS, TD, MSC
Obtained funding: Not applicable
Overall responsibility: TD, MSC
EL and AK contributed equally to this article and share co-first authorship.
TD and MSC contributed equally to this article and share senior authorship.

DISCLOSURES

M.S.C. and T.D. are co-inventors on US Patents Nos. 9,463,177 and 10,111,847 assigned to the University of California and Brigham and Womens Hospital. M.S.C. and T.D. are co-founders of VasaRx.

REFERENCES

1. Conte MS, Bradbury AW, Kolh P, et al. Global vascular guidelines on the management of chronic limb-threatening ischemia. J Vasc Surg 2019;69:3S-125S.e40.
2. Criqui MH. Peripheral arterial disease — epidemiological aspects. Vasc Med 2001;6:3-7.
3. Shu J, Santulli G. Update on peripheral artery disease: epidemiology and evidence-based facts. Atherosclerosis 2018;275:379-81.
4. Song P, Rudan D, Zhu Y, et al. Global, regional, and national prevalence and risk factors for peripheral artery disease in 2015: an updated systematic review and analysis. Lancet Glob Health 2019;7:e1020-30.
5. Hiramoto JS, Teraa M, de Borst GJ, Conte MS. Interventions for lower extremity peripheral artery disease. Nat Rev Cardiol 2018;15:332-50.
6. Shah PK. Inflammation, neointimal hyperplasia, and restenosis: as the leukocytes roll, the arteries thicken. Circulation 2003;107:2175-7.
7. Inoue T, Croce K, Morooka T, Sakuma M, Node K, Simon DI. Vascular inflammation and repair. JACC Cardiovasc Interv 2011;4:1057-66.
8. Lacolley P, Regnault V, Nicoletti A, Li Z, Michel JB. The vascular smooth muscle cell in arterial pathology: a cell that can take on multiple roles. Cardiovasc Res 2012;95:194-204.
9. Werz O, Gerstmeier J, Libreros S, et al. Human macrophages differentially produce specific resolvin or leukotriene signals that depend on bacterial pathogenicity. Nat Commun 2018;9:59.
10. Motwani MP, Colas RA, George MJ, et al. Pro-resolving mediators promote resolution in a human skin model of UV-killed Escherichia coli—driven acute inflammation. JCI Insight 2018;3:e94463.
11. Kim AS, Conte MS. Specialized pro-resolving lipid mediators in cardiovascular disease, diagnosis, and therapy. Adv Drug Deliv Rev 2020;159:170-9.
12. Serhan CN. Pro-resolving lipid mediators are leads for resolution physiology. Nature 2014;510:92-101.
13. Chiang N, Serhan CN. Structural elucidation and physiologic functions of specialized pro-resolving mediators and their receptors. Mol Aspects Med 2017;58:114-29.
14. Khoury MK, Yang H, Liu B. Macrophage biology in cardiovascular diseases. Arterioscler Thromb Vasc Biol 2021;41:e77-81.
15. Uleman JF, Mancini E, Al-Shama RFM, Te Velde AA, Kraneveld AD, Castiglione F. A multiscale hybrid model for exploring the effect of Resolvin D1 on macrophage polarization during acute inflammation. Math Biosci 2023;359:108997.
16. Serhan CN, Chiang N. Resolvins and cysteinyl-containing pro-resolving mediators activate resolution of infectious inflammation and tissue regeneration. Prostaglandins Other Lipid Mediat 2023;166:106718.
17. Wang YH, Tang YR, Gao X, et al. Aspirin-triggered Resolvin D1 ameliorates activation of the NLRP3 inflammasome via induction of autophagy in a rat model of neuropathic pain. Front Pharmacol 2023;14:971136.
18. Paz-García M, Povo-Retana A, Jaén RI, et al. Beneficial effect of TLR4 blockade by a specific aptamer antagonist after acute myocardial infarction. Biomed Pharmacother Biomedecine Pharmacother 2023;158:114214.
19. Wang L, Li J, Liao R, et al. Resolvin D1 attenuates sepsis induced acute kidney injury targeting mitochondria and NF-κB signaling pathway. Heliyon 2022;8:e12269.
20. Guilherme RF, Silva JBNF, Waclawiack I, et al. Pleiotropic antifibrotic actions of aspirin-triggered resolvin D1 in the lungs. Front Immunol 2023;14:886601.
21. Sun C, Zheng W, Liang L, et al. Acute coronary syndrome may be associated with decreased resolvin D1-to-leukotriene B4 ratio. Int Heart J 2023;64:22-7.
22. Wu B, Mottola G, Chatterjee A, et al. Perivascular delivery of resolvin D1 inhibits neointimal hyperplasia in a rat model of arterial injury. J Vasc Surg 2017;65:207-17.e3.
23. Miyahara T, Runge S, Chatterjee A, et al. D-series resolvin attenuates vascular smooth muscle cell activation and neointimal hyperplasia following vascular injury. FASEB J 2013;27:2220-32.
24. Wu B, Werlin EC, Chen M, et al. Perivascular delivery of resolvin D1 inhibits neointimal hyperplasia in a rabbit vein graft model. J Vasc Surg 2018;68:188S-200S.e4.
25. Sun YP, Oh SF, Uddin J, et al. Resolvin D1 and its aspirin-triggered 17 *R* epimer: stereochemical assignments, anti-inflammatory properties, and enzymatic inactivation. J Biol Chem 2007;282:9323-34.
26. Orr SK, Colas RA, Dalli J, Chiang N, Serhan CN. Proresolving actions of a new resolvin D1 analog mimetic qualifies as an immunoresolvent. Am J Physiol Lung Cell Mol Physiol 2015;308:L904-11.
27. Mottola G, Chatterjee A, Wu B, Chen M, Conte MS. Aspirin-triggered resolvin D1 attenuates PDGF-induced vascular smooth muscle cell migration via the cyclic adenosine monophosphate/protein kinase A (cAMP/PKA) pathway. PLoS One 2017;12:e0174936.

28. Kim AS, Werlin EC, Kagaya H, et al. 17R/S-Benzo-RvD1, a synthetic resolvin D1 analogue, attenuates neointimal hyperplasia in a rat model of acute vascular injury. PLoS One 2022;17:e0264217.
29. Friedman AD, Claypool SE, Liu R. The smart targeting of nanoparticles. Curr Pharm Des 2013;19:6315-29.
30. Cervadoro A, Palomba R, Vergaro G, et al. Targeting inflammation with nanosized drug delivery platforms in cardiovascular diseases: immune cell modulation in atherosclerosis. Front Bioeng Biotechnol 2018;6:177.
31. Kadam RS, Bourne DWA, Kompella UB. Nano-advantage in enhanced drug delivery with biodegradable nanoparticles: contribution of reduced clearance. Drug Metab Dispos Biol Fate Chem 2012;40:1380-8.
32. Dadwal A, Baldi A, Kumar Narang R. Nanoparticles as carriers for drug delivery in cancer. Artif Cells Nanomedicine Biotechnol 2018;46:295-305.
33. Brannon ER, Guevara MV, Pacifici NJ, Lee JK, Lewis JS, Eniola-Adefeso O. Polymeric particle-based therapies for acute inflammatory diseases. Nat Rev Mater 2022;7:796-813.
34. Morgan CE, Dombrowski AW, Rubert Pérez CM, et al. Tissue-factor targeted peptide amphiphile nanofibers as an injectable therapy to control hemorrhage. ACS Nano 2016;10:899-909. doi: 10.1021/acsnano.5b06025.
35. Wang GJ, Sui XX, Simosa HF, Jain MK, Altieri DC, Conte MS. Regulation of vein graft hyperplasia by survivin, an inhibitor of apoptosis protein. Arterioscler Thromb Vasc Biol 2005;25:2081-7.
36. Dalli J, Colas RA, Walker ME, Serhan CN. Lipid mediator metabolomics via LC-MS/MS profiling and analysis. Methods Mol Biol Clifton NJ 2018;1730:59-72.
37. jin Jeong W, Bu J, Kubiatowicz LJ, Chen SS, Kim Y, Hong S. Peptide—nanoparticle conjugates: a next generation of diagnostic and therapeutic platforms? Nano Converg 2018;5:38.
38. Swider E, Koshkina O, Tel J, Cruz LJ, de Vries IJM, Srinivas M. Customizing poly(lactic-co-glycolic acid) particles for biomedical applications. Acta Biomater 2018;73:38-51.
39. Bradbury AW, Adam DJ, Bell J, et al. Bypass versus Angioplasty in Severe Ischaemia of the Leg (BASIL) trial: a survival prediction model to facilitate clinical decision making. J Vasc Surg 2010;51:52S-68S.
40. Conte MS, Bandyk DF, Clowes AW, et al. Results of PREVENT III: a multicenter, randomized trial of edifoligide for the prevention of vein graft failure in lower extremity bypass surgery. J Vasc Surg 2006;43:742-51.e1.
41. Katsanos K, Spiliopoulos S, Kitrou P, Krokidis M, Karnabatidis D. Risk of death following application of paclitaxel-coated balloons and stents in the femoropopliteal artery of the leg: a systematic review and meta-analysis of randomized controlled trials. J Am Heart Assoc 2018;7:e011245.
42. Serhan CN. Resolution phase of inflammation: novel endogenous anti-inflammatory and proresolving lipid mediators and pathways. Annu Rev Immunol 2007;25:101-37.
43. Bannenberg GL, Chiang N, Ariel A, et al. Molecular circuits of resolution: formation and actions of resolvins and protectins. J Immunol 2005;174:4345-55.
44. Spite M, Clària J, Serhan CN. Resolvins, specialized proresolving lipid mediators, and their potential roles in metabolic diseases. Cell Metab 2014;19:21-36.
45. Hasturk H, Abdallah R, Kantarci A, et al. Resolvin E1 (RvE1) attenuates atherosclerotic plaque formation in diet and inflammation-induced atherogenesis. Arterioscler Thromb Vasc Biol 2015;35:1123-33.
46. Spite M, Norling LV, Summers L, et al. Resolvin D2 is a potent regulator of leukocytes and controls microbial sepsis. Nature 2009;461:1287-91.
47. Viola JR, Lemnitzer P, Jansen Y, et al. Resolving lipid mediators maresin 1 and resolvin D2 prevent atheroprogression in mice. Circ Res 2016;119:1030-8.
48. Akagi D, Chen M, Toy R, Chatterjee A, Conte MS. Systemic delivery of proresolving lipid mediators resolvin D2 and maresin 1 attenuates intimal hyperplasia in mice. FASEB J 2015;29:2504-13.
49. Makino Y, Miyahara T, Nitta J, et al. Proresolving lipid mediators resolvin D1 and protectin D1 isomer attenuate neointimal hyperplasia in the rat carotid artery balloon injury model. J Surg Res 2019;233:104-10.
50. Petri MH, Laguna-Fernandez A, Tseng CN, Hedin U, Perretti M, Bäck M. Aspirin-triggered 15-epi-lipoxin A4 signals through FPR2/ALX in vascular smooth muscle cells and protects against intimal hyperplasia after carotid ligation. Int J Cardiol 2015;179:370-2.
51. Zhang MJ, Sansbury BE, Hellmann J, et al. Resolvin D2 enhances postischemic revascularization while resolving inflammation. Circulation 2016;134:666-80.
52. Davies MG, Hagen PO. Pathobiology of intimal hyperplasia. Br J Surg 1994;81:1254-69.
53. Schwartz SM. Smooth muscle migration in atherosclerosis and restenosis. J Clin Invest 1997;100:S87-9.
54. Kerimoglu O, Alarcin E. Poly(Lactic-Co-Glycolic acid) based drug delivery devices for tissue engineering and regenerative medicine. ANKEM Derg 2012;26:86-98.
55. Wessely R. New drug-eluting stent concepts. Nat Rev Cardiol 2010;7:194-203.
56. Fredman G, Kamaly N, Spolitu S, et al. Targeted nanoparticles containing the proresolving peptide Ac2-26 protect against advanced atherosclerosis in hypercholesterolemic mice. Sci Transl Med 2015;7:275ra20.
57. Norling LV, Spite M, Yang R, Flower RJ, Perretti M, Serhan CN. Cutting edge: humanized nano-proresolving medicines mimic inflammation-resolution and enhance wound healing. J Immunol 2011;186:5543-7.

Submitted Apr 22, 2023; accepted Aug 17, 2023.